Compensating for pose and illumination in unconstrained periocular biometrics

Chandrashekhar N. Padole and
Hugo Proença*

Department of Computer Science,
IT – Instituto de Telecomunicações,
University of Beira Interior,
6200-Covilhã, Portugal
Fax: +351-275-319899
E-mail: chandupadole@ubi.pt
E-mail: hugomcp@di.ubi.pt
*Corresponding author

Abstract: In the context of *less constrained* biometrics recognition, the use of information from the vicinity of the eyes (periocular) is considered with high potential and motivated several recent proposals. In this paper, we focus on two factors that are known to degrade the performance of periocular recognition: varying illumination conditions and subjects pose. Hence, this paper has three major purposes: 1) describe the decreases in performance due to varying illumination and subjects poses; 2) propose two techniques to improve the robustness to these factors; 3) announce the availability of an annotated dataset of periocular data (UBIPosePr), where poses vary in regular intervals, turning it especially suitable to assess the effects of misalignments between camera and subjects in periocular recognition.

Keywords: unconstrained biometrics; periocular recognition; illumination compensation; pose compensation; pose estimation.

Reference to this paper should be made as follows: Padole, C.N. and Proença, H. (2013) 'Compensating for pose and illumination in unconstrained periocular biometrics', *Int. J. Biometrics*, Vol. 5, Nos. 3/4, pp.336–359.

Biographical notes: Chandrashekhar N. Padole received his BE in Electronics Engineering from the Nagpur University, Nagpur, India, in 1997. He received his ME in Electronics Engineering from the Mumbai University, Mumbai, India in 2002. Currently, he is working towards his PhD degree in the area of unconstrained biometrics and is a member of NECOVID project team in University of Beira Interior, Covilhã, Portugal. In his research career, he was associated with Biomedical Engineering Department of IIT Bombay, Powai, Mumbai as a Research Scholar from 2002 to 2005 and with R&D cell of KPIT Cummins Infosystems Ltd., Pune, India as a Sr. Research Associate from 2007 to 2009. He also worked for the research project 'BioRec' at the SOCIA Lab, University of Beira Interior, Covilhã. He has authored around ten research papers in international conferences. His research interests include signal and image processing, computer vision and pattern recognition, computational intelligence and biometric systems.

Hugo Proença received his BSc in Mathematics/Informatics from the University of Beira Interior (UBI), Covilhã, Portugal, in 2001, MSc degree from the Faculty of Engineering, University of Oporto, in 2004, and PhD in Computer Science and Engineering from UBI, in 2007. His research interests are artificial intelligence, pattern recognition and computer vision, with emphasis to biometrics, less constrained iris recognition systems. Currently, he serves as an Assistant Professor in the Department of Computer Science, UBI. He is the author of over 50 publications. He is the Associate Editor (for ocular biometrics area) of the *IEEE Biometrics Compendium Journal* and member of the editorial board of the *International Journal of Biometrics*. Also, he served as the Guest-Editor of special issues of the pattern recognition letters, image and vision computing and signal, image and video processing journals.

1 Introduction

Biometrics is considered a successful case of pattern recognition systems and is used for multiple purposes: authentication in restricted areas, attendance record in office premises, citizenship recognition and forensics. Among different possibilities, the iris trait is one of the most popular and several works were published in this scope, either focused in the segmentation, encoding, image enhancement and fusion strategies (e.g., Srividya et al., 2009; Jia et al., 2012; Thangasamy and Latha, 2012). However, when it comes to usability, systems still operate in constrained data acquisition scenarios, which justifies the growing efforts in strategies to reduce the constraints of the data acquisition phase [*non-cooperative* systems (Savvides et al., 2010; Selvan and Sulochana, 2010; Du and Yang, 2012)]. The main hurdles are the decreases in data quality due to large camera-subject distances and its non-uniformity in terms of factors such as translation, rotation, scale, pose and illumination. In this context, the term *periocular biometrics* has emerged and refers to the recognition using information from the "facial region in the immediate vicinity of the eye" (Park et al., 2011). Park et al. (2012) discussed the challenges of recognition in non-ideal data and the impact of camera-subject distance was reported by Bharadwaj et al. (2010).

The work described in this paper can be summarised as follows:

1 we assess the decreases in performance with respect to two criteria: lighting conditions and subjects poses, regarded as covariates of performance

2 propose methods to compensate for these, consistently improving the recognition effectiveness.

For such, we acquired and manually annotated a dataset (UBIPosePr), that contains subjects with varying poses and under both natural and artificial varying light sources.

These are the remaining parts of this paper: Section 2 overviews the related literature. The description of the pose and illumination problems appears in Section 3. Section 4 describes the technique that compensates for illumination and Section 5 the technique used to compensate for pose. A description on the newly acquired dataset is found in

Section 7. The experimental results and corresponding discussion are given in Section 8. Finally, the paper is concluded in Section 9.

2 Related work

For comprehensibility, our analysis of the related work was divided into three parts:

1 periocular biometrics

2 illumination compensation methods

3 pose estimation/compensation techniques.

2.1 Periocular biometrics

The use of other traits in the ocular area apart the iris has been the scope of different research works (e.g., Juhola et al., 2012).

Park et al. (2009) highlighted the advantages of using the periocular region, when compared to the exclusive use of the iris. The periocular texture was characterised by local binary patterns (LBP), histograms of oriented gradients (HOG) and scale invariant feature transform (SIFT). Variations in performance with respect to the inclusion of eyebrows in the region-of-interest were also reported. In a subsequent work (Park et al., 2011), authors focused on other factors that affect performance, such as segmentation inaccuracies, partial occlusions and pose. Experiments were carried in the FRGC 2.0 database (NIST, http://www.frvt.org/FRGC/). Having soft biometric purposes, Lyle et al. (2010) classified gender and ethnicity from periocular data, using LBP features to feed a support vector machine. A noteworthy conclusion was that effectiveness yielded when using exclusively periocular data is comparable to the obtained by using the entire face. Woodard et al. (2010) studied the effect of fusion techniques on periocular and iris data on non-ideal scenarios, characterised by occluded irises, motion and spatial blur, poor contrast and illumination artefacts, having concluded that fusion at the score level improves performance. Simpson et al. (2010) applied genetic and evolutionary computations (GEC) to the feature selection problem, having compared two GEC-based Type-II feature extraction methods: a steady-state genetic algorithm and an elitist estimation of distribution algorithm. The latter not only optimised accuracy but also minimised the dimensionality.

Bharadwaj et al. (2010) used visible light data, fusing of a global matcher (spatial envelope) and circular linear binary patterns. Also, authors investigated the effect of acquisition distance on performance, having used the UBIRIS.v2 database (Proença et al., 2010). Aiming at robustness, Miller et al. (2010) assessed the linear correlation between image quality and performance. Recently, Park et al. (2012) handled non-ideal ocular data and discussed the challenges around deformations and varying illumination in samples. To overcome these issues, authors proposed probabilistic deformation models, having used a maximum-a-posteriori estimation filter in the fusion of HOG, SIFT-based and probabilistic density model based scores, yielding a technique that was favourably compared to the non-weighted score level fusion. Hollingsworth et al. (2012) compared the recognition ability of humans and machines on periocular data, concluding that – at

least – automated strategies have similar effectiveness to humans. Juefei-Xu et al. (2011) discussed the use of local descriptors along with pose correction and illumination normalisation techniques. The experiments were carried in the FG-NET database. A similar study of the same authors is reported in Juefei-Xu and Savvides (2012). Woodard et al. (2011) represented skin texture and colour separately, fusing both types of information at subsequent processing phases. Finally, Crihalmeanu and Ross (2011) fused periocular recognition techniques to methods that describe the sclera texture and vasculature patterns.

2.2 Illumination compensation

A relatively reduced number of works addressed the effect of lighting conditions in periocular recognition performance. Even though, it is considered that non-uniform illumination over a sample, or of different lighting conditions for image pairings, significantly affects performance. Juefei-Xu et al. (2011) and Juefei-Xu and Savvides (2012) used anisotropic diffusion techniques, having observed improvements in performance, even though at expenses of a substantial overload in computational requirements. Oppositely, in the field of face recognition, a large number of research works on this topic can be found: Xie et al. (2011) normalised illumination on high scale components along with slight adjustments on low scale features. Du and Ward (2010) handled the problem of side lighting effects by adaptive region-based image preprocessing techniques. After wavelet decomposition, approximation coefficients feed a region-based histogram equalisation module, while detail coefficients were modified using region based edge enhancement, yielding performance levels that match those reported by Chen et al. (2006) and Xie et al. (2008). More recently, Cheng et al. (2010) compared methods based on self-quotient image (SQI) (Wang et al., 2005), dynamic morphological quotient image (He et al., 2007) and different smoothing filters, having reported that the latter kind of techniques outperform.

2.3 Pose estimation and compensation

Storer et al. (2009) used a 3D morphable appearance model to estimate yaw and pitch angles for human heads, having authors reported estimation errors of 5 degrees at most. Liu et al. (2009) used pose-based non-negative matrix factorisation and eigen-analysis to estimate pose, reporteing average errors for yaw and tilt around 12 degrees. A multiphase head pose estimation was given by Wu and Trivedi (2008): they used Gabor features and its projections on subspaces formed by principal component analysis (PCA), kernel PCA, Fisher discriminant analysis (DA) and Kernel DA, that fed a nearest neighbour matching phase. Then, the estimation was refined using bunch graph similarity measures. Kim et al. (2005) used surface curvature and the tetrahedral structure of nose to estimate pose. Zhao and Gao (2006) obtained an estimate of pose based in elastic energy models, in the symmetry of human faces and Hooke's law of springs. A pose correction technique for local feature-based face authentication was reported by González-Jiménez et al. (2006), segmenting the prominent facial features based on the angular second moment description. Dahmane et al. (2010) detected the symmetrical parts of faces, from where yaw and pitch angles were inferred.

2.4 Non-orthogonal biometric recognition

In the case of facial recognition, several works concerned about the recognition of non-frontal or profile images: Zheng et al. (2009) recognised multi-view facial images under the unified Bayes theoretical framework, having formulated the problem as an optimisation problem of minimising an upper bound of the Bayes error. Demirel and Anbarjafari (2008) proposed a computational effective method based in probabilities distribution functions of pixels intensities in different colour speces. They were used as feature vectors by minimising the Kullback-Leibler distance between a sample and templates stored in the database. Singh et al. (2007) relied in the notion of mosaic and aligned deviated to frontal data by a hierarchical registration algorithm based on neighbourhood properties. Multi-resolution splining blend the side profiles with the frontal image, thereby generating a composite face image that is used in recognition. Wolf et al. (2011) used patch-based LBP and represented samples by a set of similarities to templates (designated *background samples*) and to prelearned classifiers of different types (linear discriminants and support vector machines). Relying on facial landmarks that are deemed to be more robust to variations in pose, Cheung et al. (2008) proposed an algorithm based on the elastic bunch graph matching algorithm, having concluded about its robustness in case of deviations up to 30 degrees in absolute value.

Constituting a much more matured field of knowledge and sharing the region-of-interest where recognition is performed, iris biometrics techniques are closely related to periocular recognition. Being a small moving target, appropriate strategies to handle off-angle iris data were the scope of various works, where most techniques estimate gaze by 3D projection techniques, maximising the response of the Daugman's integro-differential operator (e.g., Dorairaj et al., 2005; Schmid et al., 2010) or the length of the axes of an iris bounding ellipse (e.g., Zuo and Schmid, 2009). In a different paradigm, Abhyankar et al. (2005) designed a bi-orthogonal wavelet network, repositioned to account for deviations. Schuckers et al. (2007) used an angular deformation calibration model. The angular deformations are modelled, and calibration parameters are calculated under a supervised machine learning technique, being finally used in the projection onto the plane closest to the base plane. Chou et al. (2010) proposed a circle rectification method, estimated using the centre and axes of the segmented pupillary boundary. Then, data is stretched, so that both axis have the same length.

When it comes to periocular biometrics, the most relevant works were due to Schuckers et al. (2007) and Abhyankar et al. (2005). A bi-orthogonal wavelet network was trained from a learning set. Probes were repositioned for different angles and their Euclidean distance to gallery data obtained, considering the minimum distance as the matching score. Also, authors worked on two other approaches:

1 gaze was estimated using Daugman's integro-differential operator as the objective function

2 an angular deformation calibration model was created and calibrated, so to estimate a frontal image used subsequently.

3 Problem description

The robustness of biometric recognition to non-ideal conditions motivated numerous research works, usually regarding such acquisition conditions as *covariates* that affect performance. Even though periocular biometrics appears to be particularly robust to such covariates, the results given in Figure 1 show an evident decrease in performance when deviations in pose occur. We plot three receiver operating characteristics curves, when matching frontal gallery data to frontal probes ('frontal' line), to slightly deviated ('deviated' line) and notoriously deviated probes ('more deviated' line). Additional details about these experiments are given here (Padole and Proença, 2012).

Figure 1 Motivation for the work described in this paper: the performance of periocular recognition in result of variations in pose remarkable decreases, in direct proportion to the magnitude of deviations (see online version for colours)

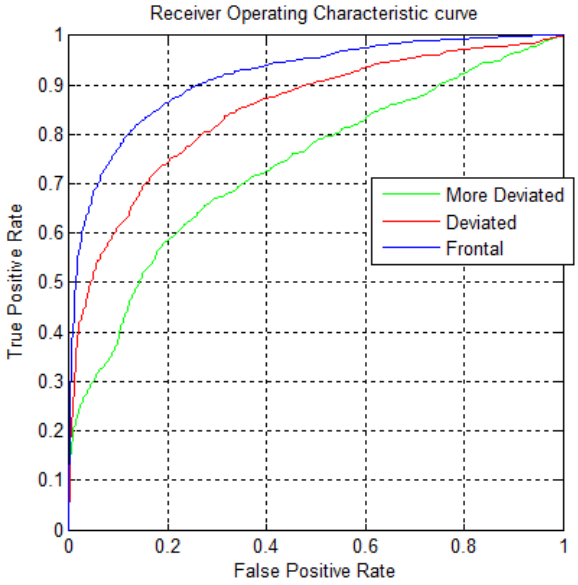

Source: Padole and Proença (2012)

Also, even considering that the feature descriptors usual in periocular recognition (LBPs, HOGs and SIFT) tend to be invariant to uniform (global) changes in illumination, they are not invariant to non-uniform (local) changes. Plus, multiple light sources in the environment and the periocular morphology might easily lead to the existence of umbra and penumbra regions, which dramatically change the appearance of the periocular skin texture. According to these motivations, we tested two different techniques to compensate for lighting conditions:

1 homomorphic filters (Gonzalez and Woods, 1992), selected over anisotropic diffusion due of their lower computational complexity

2 the SQI (Wang et al., 2004), selected among a family of quotient-image variants, due to the fact of being possible to obtain from a single image.

In order to compensate for pose, a method based on projective transforms is proposed. When acquiring with a perspective camera, projective transform (also called a homography or collineation) preserves both singularities and multiplicities and the corresponding matrix can be derived from 3D angles associated with pose variations. A contribution of this work is to deem the optimal projective transform matrix from a set of landmarks: in order to align probes to gallery data as much as possible. A high-level perspective of the proposed workflow is depicted in Figure 2. At this point, it should be stressed that the novelty of the proposed technique is not the use of projective transforms to compensate for deviations, but the method that finds the optimal transform: we rely exclusively on the eye corners, which are the most easily distinguishable landmarks in the periocular region. Hence, when using exclusively an estimate of both eye-corners, we define a quadrilateral that is used as goodness function among different possibilities for projective transforms.

Figure 2 Workflow diagram of the proposed techniques to compensate for illumination conditions and varying poses

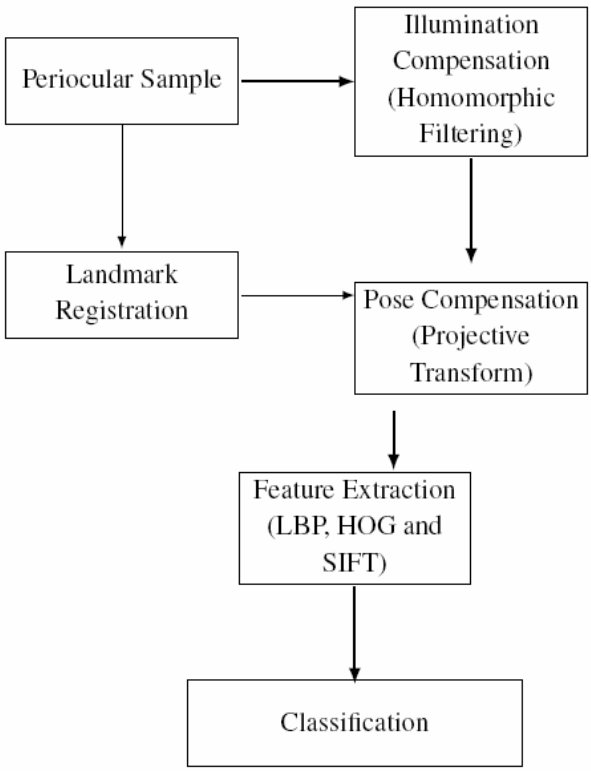

4 Illumination compensation

Even in non-controlled acquisition environments, a reasonable assumption is that the illumination varies slowly across the image, in opposition to objects' reflectance that varies much more rapidly. This gave birth to the idea of a frequency-domain non-linear

filter that reduces intensity variations across the image while highlighting detail. Homomorphic filters are frequently used in different image processing applications, especially due to their low computational complexity, which was one of the main reasons to select them for the scope of this work. A homomorphic filtering operation starts by expressing an image by the product of illumination I and reflectance R. It is given by:

$$I_h(x, y) = \exp\left(F^{-1}\left(H \cdot I_f\right) + F^{-1}\left(H \cdot R_f\right)\right) \tag{1}$$

where $F(.)$ denotes the Fourier transform, F^{-1} its inverse, $I_f = F(\ln(I + 1))$ is the image represented in the frequency domain and $R_f = F(\ln(R + 1))$ denotes the reflectance in the frequency domain. H is the Butterworth high pass filter and $I_h(x, y)$ is the filtered image. Also, we tested a variation of the widely used quotient image technique, described by Shashua and Riklin-Raviv (2001). In this case, the SQI, as proposed by Wang et al. (2004), was chosen, due to the fact of obtaining an illumination normalised version from a single image, which is of obvious interest for our purposes. The point-by-point proportion between an image and its smoothed version gives the SQI:

$$Q(x, y) = \frac{I(x, y)}{F(x, y) * I(x, y)}, \tag{2}$$

where $I(x, y)$ is the original image, $F(x, y)$ is a smoothing filter and '*' is the convolution operator. $Q(x, y)$ is invariant to illumination under the assumptions that the strength and direction of the light sources are uniform across the image and the normal to the object is locally uniform. Additional details can be found at Wang et al. (2004).

5 Pose compensation

When an object changes its position in the scene, a homography maps such transformation that might include changes in scale, rotation, translation and sheer. Hence, the deflection in any point with respect to the world coordinate system can be transformed to image plane using the projective transform represented in homogeneous notation:

$$\lambda \begin{bmatrix} x \\ y \\ 1 \end{bmatrix} = \begin{bmatrix} h_{11} & h_{12} & h_{13} \\ h_{21} & h_{22} & h_{23} \\ h_{31} & h_{32} & h_{33} \end{bmatrix} \begin{bmatrix} X \\ Y \\ Z \end{bmatrix}, \tag{3}$$

where $\lambda = f/Z$, being f the focal length, X, Y and Z the world coordinates and x, y and z the image coordinates (Paul, 1989). When the pose of a given object varies, the associated transformation in the world coordinate system is mapped into the image, in order to recover the pre-distortion state. The 2D projective mapping has 8 degrees-of-freedom, and these values can be determined from a minimum of four pairs of point correspondences, that constitute the corners of a quadrilateral in the reference and distorted images. Let $(x_k, y_k) \rightarrow (x'_k, y'_k)$, $k = \{1, 2, 3, 4\}$ denote such correspondences, exemplified in Figure 3. A projective transformation matrix H can be determined uniquely *if and only if* no three points are collinear.

Figure 3 Illustration of landmarks correspondences in the reference and distorted samples

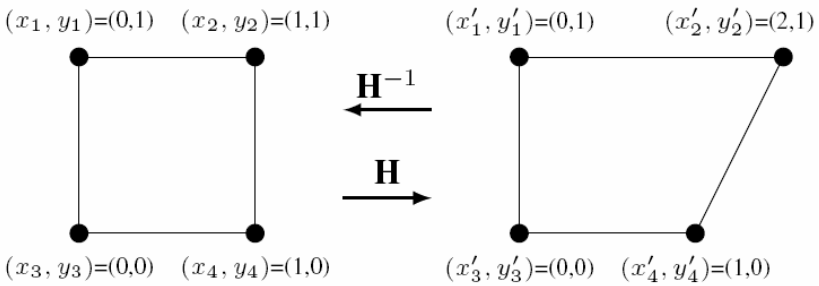

Notes: Here, only one of the corners of the quadrilateral changed its position. A projective transform H and its inverse are able to map between both samples.

The four landmarks correspondences can be combined in matrix form:

$$\begin{bmatrix} x_1 & y_1 & 1 & 0 & 0 & 0 & -x_1'x_1 & -x_1'y_1 & -x_1' \\ 0 & 0 & 0 & x_1 & y_1 & 1 & -y_1'x_1 & -y_1'y_1 & -y_1' \\ x_2 & y_2 & 1 & 0 & 0 & 0 & -x_2'x_2 & -x_2'y_2 & -x_2' \\ 0 & 0 & 0 & x_2 & y_2 & 1 & -y_2'x_2 & -y_2'y_2 & -y_2' \\ x_3 & y_3 & 1 & 0 & 0 & 0 & -x_3'x_3 & -x_3'y_3 & -x_3' \\ 0 & 0 & 0 & x_3 & y_3 & 1 & -y_3'x_3 & -y_3'y_3 & -y_3' \\ x_4 & y_4 & 1 & 0 & 0 & 0 & -x_4'x_4 & -x_4'y_4 & -x_4' \\ 0 & 0 & 0 & x_4 & y_4 & 1 & -y_4'x_4 & -y_4'y_4 & -y_4' \end{bmatrix} hH = 0 \tag{4}$$

which has the form $A_h = 0$. The solution h is the (one dimensional) *null* space of A and corresponds to the projective transform H in vector form.

Figure 4 Location of landmarks (eye centre and eye corners) in the periocular region, defining a region of interest with respect to eye's centre and width (see online version for colours)

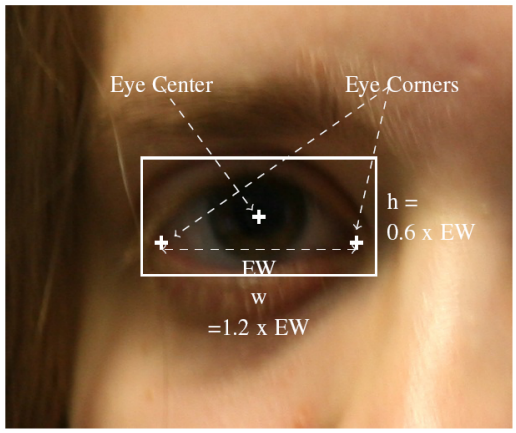

6 Proposed optimisation procedure

Empirically, we observed that even small errors in the location of landmarks correspondences have a large effect in the projective transform found and in the resulting image compensated for pose. Hence, we devised an alignment process composed by three main phases:

1 At first, we relied on eye-corners, which are known to be among the most distinguishable landmarks inside the periocular region [a detection method proposed by Santos and Proença (2011) was used].

2 The eye centre e_c was estimated from the geometric mean of both corners. The distance between eye-corners is used to draw a rectangle of dimensions $0.6\ e_w \times 1.2\ e_w$, centred at $((x_1 + x_2) / 2, (y_1 + y_2) / 2)$ and then shifted by $(0, 0.1\ e_w)$, being (x_1, y_1) and (x_2, y_2) the coordinates of both eye-corners. These values were used to define the vertices of a quadrilateral, with dimensions proportional to the eye width, as shown in Figure 4.

3 An optimisation process was carried out by slightly deviating some vertices of this quadrilateral, obtaining successive values of a cost function that under minimisation yielded the optimal projective transform.

For each probe, several projective transforms were evaluated by a cost function that measures the similarity between gallery data and the transformed probe. Then, the projective transform that attains maximal similarity corresponds to the optimal alignment procedure between. Similarity was measured in different feature subspaces, using the Chi-square distance between gallery and probe feature vectors. A cohesive perspective of the optimisation procedure is given in Figure 5.

Formally, let $A_i = (x_i, y_i)$ be a point at column x and row y. $R(A_i, A_j, A_k, A_m)$ is a polygon with vertices (A_i, A_j, A_k, A_m) over the eye region. Upon the constraints that $y_i = y_j$, $x_j = x_k$, $y_k = y_m$ and $x_m = x_i$, this region defines a rectangle centred at the geometric mean of the eye corner, as proposed in Padole and Proença (2012). Let $R^G(A_1, A_2, A_3, {}_{A4})$ be a rectangle inside the gallery image. Similarly, let $R^P(A_i, A_j, A_k, A_m)$ be the polygon extracted from the pose deviated sample. After registering landmarks, data is resized to the gallery size, in order to compensate for changes in scale and translation (Figure 6). Next, a set of projective transform matrices was generated (as per computational complexity that is affordable), using these landmark correspondences and slight variations in each vertex (moving each in a neighbourhood of radius r). We select the projective transform matrix that minimises the pairings dissimilarity in one of the feature spaces described below. Using pixelsÕ intensity, LBPs and HOGs to describe the periocular texture, the mean-squared point-by-point distance was used to measure dissimilarity:

$$f_D\left(R^P, R^G\right) = \frac{1}{L}\sqrt{\sum_{k=0}^{L-1}\left[F_G(k) - F_P(k)\right]^2}, \tag{5}$$

where $F_G(k)$ and $F_P(k)$ are the feature representation inside the gallery and probe data and L is the dimension of the feature space. Finally, the projective transform selected is given by:

$$H^* = \arg\min_{H} f_D[.,.]. \tag{6}$$

Figure 5 Cohesive perspective of the pose compensation process

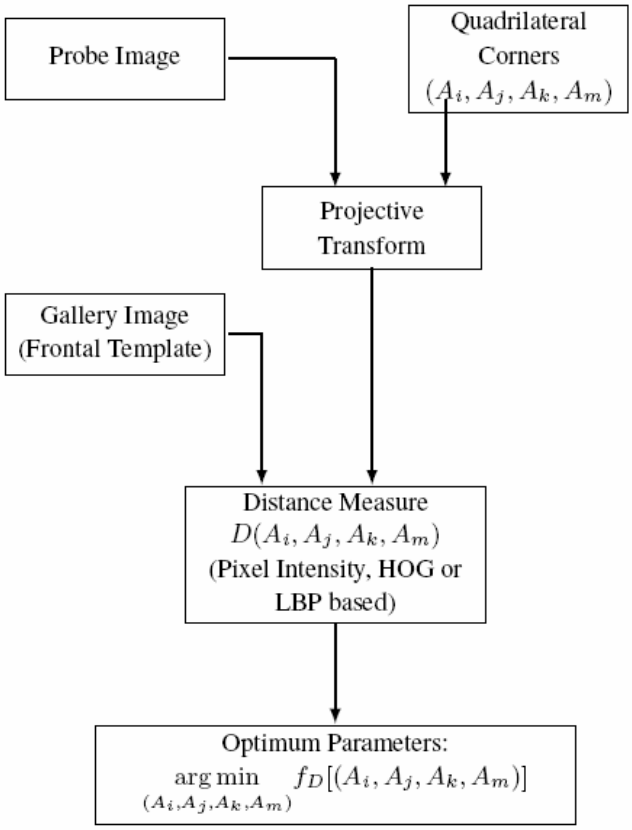

Note: The projective transform that minimises the distance between the probe data and the set of gallery samples is deemed to represent the optimal alignment process and used in subsequent processing phases.

Figure 6 Landmarks correspondences in the (a) quadrilateral ROIs on the gallery and (b) probe images

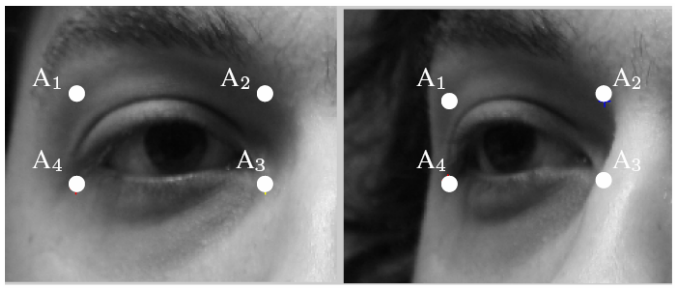

(a) (b)

In our experiments, for computational purposes we used a hierarchic search scheme to avoid the exhaustive computation of all possibilities in a range. In the earliest version of our experiments, we changed all vertices and the corresponding optimisation procedure took several hours to be carried out per image. Next, we varied exclusively one corner of the quadrilateral and noticed that the obtained results were quite close in terms of the final recognition performance. Hence, only landmark deviations at one side of the quadrilateral were tested (for vertices A_2 and A_3 in Figure 6).

7 Dataset description

The UBIPosePr dataset is freely available to the research community[1] and can be used for periocular recognition experiments related to pose and illumination variations. Data was acquired in two sessions at different locations with varying lighting conditions, either due to the amounts of light and types of illuminants. There are 100 subjects of varying ethnicity (96% Caucasian, 2% African and 2% Asians), gender (85% males and 15% females) and ages (mean 23.15, standard deviation 2.93 years). The acquisition setup is given in Figure 7:

- *Session I*. Six samples from each subject with frontal pose were acquired. This session was completely indoor, with overhead lamps. Subjects were at six metres away from the camera, which resulted in uniform illumination across the samples, with some poorly illuminated data.
- *Session II*. This session provided 18 samples per subject. Out of them, six samples are frontal, six samples are left deviated and six have right deviated poses. Though this session was also indoor, it was conducted near open windows, allowing natural light to reflect on subjects. The subject-to-camera distance was five meters. The pose angles were annotated, as in Murphy-Chutorian and Trivedi (2009), by placing markers on the walls and asking for subjects cooperation. The left pose set covers angles in negative degrees {–20°, –33°, –48°, –60°, –79°, –84°} and right pose comprises positive values {10°, 20°, 35°, 45°, 60°, 85°}. The fact that angles are non-symmetrical was due to physical constraints of the acquisition environment and of the acquisition setup itself.

Some examples of the dataset are shown in Figure 8, where variations in pose and illumination are evident. Additionally, there are variations in illumination between left and right eyes, which were divided into three classes:

1 Single-eye variations are due to the deeper location of eyes, surrounded by forehead, nose and cheeks. Indoor, there is a high possibility that eye regions have shadows or less illumination than skin.

2 Eye-pair variations occur when one of the eyes is more illuminated than the other due to lateral illumination.

3 Probe-gallery variations, as gallery images were captured in relatively controlled setups, and probes in unconstrained conditions.

Figure 7 Image acquisition setup for both sessions, using gaze direction markers, represented in the figure by dot black points

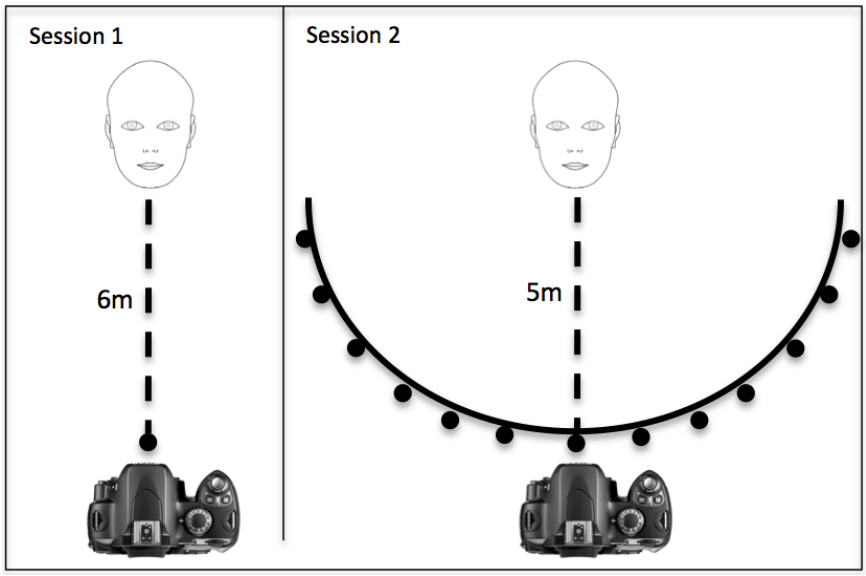

Figure 8 Sample images from the UBIPosePr dataset (see online version for colours)

Notes: Row 1: first session, frontal samples; Row 2: second session, off-angle data {–20°, –33°, –48°, –60°, –79°, –84°} degrees; Row 3: second session, frontal samples; Row 4: second session with deviation angles of {10°, 20°, 35°, 45°, 60°, 85°} degrees.

8 Experimental results

Our experiments were performed according to the periocular recognition method of Park et al. (2011) that is among the most relevant works on this subject and often used as reference term. Based on a ROI that contains the periocular region, the feature extraction process performs both local and global analysis. The ROI is divided into a grid and for each cell, both the HOG and LBP descriptors were extracted. The feature representations inside each cell are concatenated to form a global descriptor. Further, the position and scale of the interest points found by SIFT are extracted. For the resulting feature vector, the Euclidean distance is used to calculate the matching distance between global descriptors and the distance ration-matching scheme is used for the local matcher (SIFT).

8.1 Effect of illumination compensation

The improvements in performance due to the illumination compensation techniques are summarised in this section. A set of frontal images was used and divided into two groups: gallery and probe data. At first, gallery images were matched against probes without any compensation technique. Then, the experiment was repeated after preprocessing data by the techniques described in Section 4. After tuning the parameters of each method in a completely disjoint dataset, the ROC curves obtained for the test data are given in Figure 9. The error bars at each operating point give the best and worst performances observed and enable to perceive how much results vary with respect to changes in data. They resulted from repeating the experiments 20 times, randomly selecting 90% of the genuine and impostor comparisons of the complete dataset, in a bootstrapping-like strategy.

Figure 9 Improvements in performance due to illumination compensation techniques (see online version for colours)

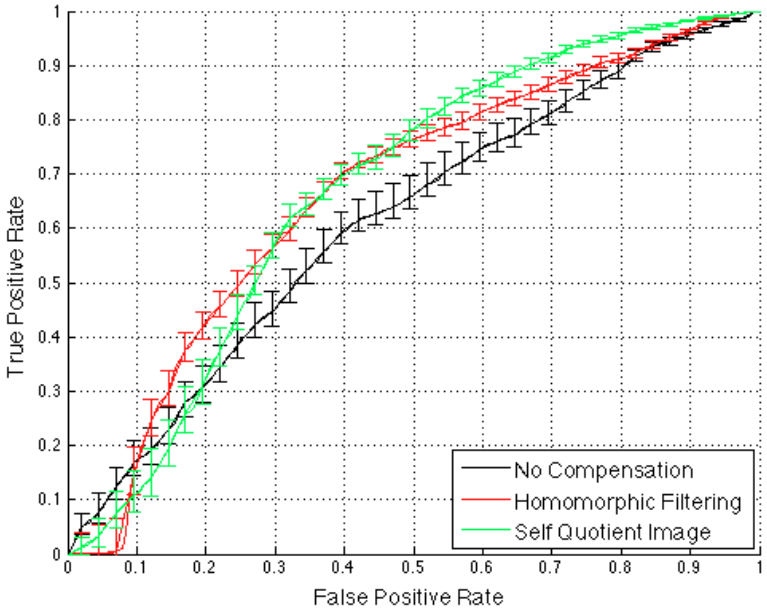

We confirmed that both homomorphic filters and the SQI contribute for the normalisation of images with respect to changes in illumination and lead to improvements in performance, when compared to the results observed without any compensation (black lines). Equal error rates (EER) observed were of about 42.6 ± 4.1% (mean ± standard deviation) when using no compensation technique and 35.0 ± 2.9 and 35.2 ± 2.8 when using the homomorphic and SQI compensation techniques. We noted that the SQI and homomorphic filters outperformed on different ranges of the performance space: the latter technique appears to be the best for high confidence recognition, where low false match rates are demanded. Oppositely, the use of the SQI might be preferable on the other extreme of the performance space, where the number of false alarms might be neglected in respect of the recognition systems' sensitivity.

8.2 Effect of pose compensation

To perceive the effect of pose in recognition performance, images were manually classified into three groups:

1 The *frontal* subset comprises samples with no deviation in pose, i.e., ≈ 0°, either from Session I or Session II. This set was further divided into two disjoint subsets: *Gallery* and *Probes*.

2 The *deviated* subset contains images with absolute pose angle less than or equal to 60°, i.e., $|\theta| \leq 60°$.

3 In the case of the *extremely deviated* subset, images have deviation angles greater than 60°, i.e., $|\theta| > 60°$.

Initially, we aimed at testing if the pose parameter actually has a statistically significant effect in the performance of periocular recognition. Hence, we devised an hypothesis test, stating as *null hypothesis* that there is no linear correlation between the scores obtained for genuine comparisons and the corresponding poses. The Pearson's coefficient measures this kind of correlation:

$$\rho(S, P) = \frac{n\sum sp - \left(\sum s\right)\left(\sum p\right)}{\sqrt{\left(n\sum s^2 - \left(\sum s\right)^2\right)\left(n\sum p^2 - \left(\sum p\right)^2\right)}}, \tag{7}$$

where S and P denote the similarity scores and absolute values of pose angles. The average scores for *genuine* comparisons with respect to pose are given in Figure 10. ρ follows a t-distribution with $n - 2$ degrees of freedom and the corresponding test statistic is given by:

$$t = \rho\sqrt{\frac{(n-2)}{1-\rho^2}}. \tag{8}$$

At a significance level of $\alpha = 0.01$, the critical t-value of 2.81 was obtained and enabled to reject the *null* hypothesis. Table 1 gives the t-values obtained for the correlation scores obtained when using the HOG, LBP and SIFT feature descriptors. Being consistently larger that the critical value (≈ 9.11), the *null* hypothesis was clearly rejected in all cases. Therefore, as the final matching score is a linear combination of HOG, LBP and SIFT

scores, we concluded that pose affects the scores of genuine comparisons and – this way – degrades recognition performance.

Figure 10 Normalised average similarity scores of the genuine comparisons with respect to deviations in pose and for different feature descriptors (see online version for colours)

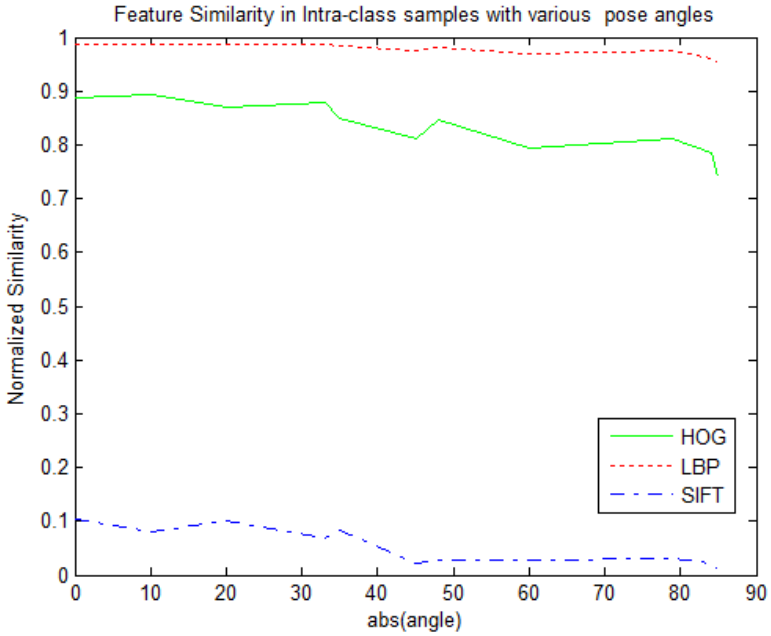

Notes: LBPs and SIFT showed a more robust behaviour to deviations in pose, whereas HOGs almost linearly decreased their average similarity with respect to deviation angles. Note that in this analysis, the flatness of lines should be regarded, instead of their absolute value.

Table 1 Results of hypothesis testing

Descriptor	*ρ*	*t-value*	*Result*
HOG	89.80	9.111	Reject
LBP	13.34	9.136	Reject
SIFT	$1.86e^5$	9.110	Reject

To assess the improvements in performance due to the proposed pose compensation strategy, a comparison between frontal gallery data and probes of varying pose was carried out. At first, we observed the results without any pose compensation technique. Next, we repeated the experiments when compensating for pose. Results are given in Figure 11, where the black lines denote no pose compensation and the red, green, and blue lines denote the results when compensating for pose using each of the tested optimisation strategies. The left plot gives the results for *deviated* data, whereas the right plot shows the corresponding values for *extremely deviated* data. The error bars at each operating point give the best and worst observed performance and enable to perceive how much results will vary with respect to changes in data. They were obtained when

repeating the recognition experiments 20 times, randomly selecting 90% of the genuine and impostor comparisons, in a bootstrapping-like strategy.

In the case of deviated data, the EER observed were of about 41.3 ± 3.1% (mean ± standard deviation) when using no pose compensation technique and 42.1 ± 2.8, 40.7 ± 2.1 and 36.3 ± 1.8%when using the proposed compensation strategy, according to the intensity, LBP and HOG optimisation criteria. Regarding extremely deviated data, the corresponding EER values were of about 45.1 ± 0.9% without any compensation technique and of 45.3 ± 0.4, 46.1 ± 0.6 and 41.0 ± 0.8 with the intensity, LBP and HOG optimisation criteria. It is obvious that pose compensation improves performance in the case of *deviated* samples, but only marginal improvements were observed for *extremely deviated* data. Here, it is interesting to observe the poor levels of performance for this type of data, which was justified by the non-planar shape of the periocular region that leads to occlusions in case of extreme deviations (over 60° in absolute value), that cannot be recovered by single camera projection techniques. For both the *deviated* and *extremely deviated* cases, the pose compensation technique yielded best performance when using the HOG descriptors in the optimisation process. In this case, apart from observing the best performance values, their variation was also the smallest (note the amplitude of error bars), which was positively regarded.

Having concluded positively about the improvements in performance due to pose compensation when handling *deviated* samples (with misalignments lower than 60° in terms of absolute value), it is equally important to test whether the proposed method decreases the performance yielded for aligned data. Table 2 summarises the observed area under curve (AUC) values, giving the values obtained when using exclusively one of the eyes (R = right and L = left), and both eyes (RL), for each kind of feature descriptors (HOG, LBP and SIFT), and when fusing them at the score level (fusion). Also, values are shown for three sub sets (frontal, deviated and extremely deviated data). It can be confirmed that in no case the proposed method contributed for decreases in performance. Oppositely, compensating for pose consistently improved performance in the case of deviated data, which was regarded as an achievement.

A noteworthy discussion is about the levels of performance observed, that are lower than the reported in previous works, such as those in Figure 1. However, it should be stressed that the quality of the data used in far worse in the case of our experiments, which was also a purpose of this work, to obtain a lower bound for the performance in such bad quality data. Hence, we claim that the given results are meaningful in relative terms and not in terms of the absolute values.

Figure 12 summarises the improvements in performance due to the pose compensation techniques. The vertical axis represents variations in recognition sensitivity (TPR) and the horizontal axis the compensation technique used. The left plot regards the techniques used to compensate for illumination, giving the variations in sensitivity when compared to not using any illumination compensation technique. Plots at the centre and right give the variations in sensitivity observed when using the proposed technique to compensate for pose with respect to not using any compensation strategy. The centre plot regards *deviated* data and the plot at right regards *extremely deviated data*. For each plot, we give the values observed when using all the techniques tested in this paper:

1 for illumination compensation, the homomorphic filtering and SQI

2 for pose compensation, the three optimisation variants: pixel intensity, HOG and BP.

Figure 11 Comparison between the ROCs obtained when no pose compensation is performed ('no compensation' lines) and when compensating for pose according to three optimisation variants: based on pixel intensity, HOG and LBP, (a) the deviated subset (b) extremely deviated data (see online version for colours)

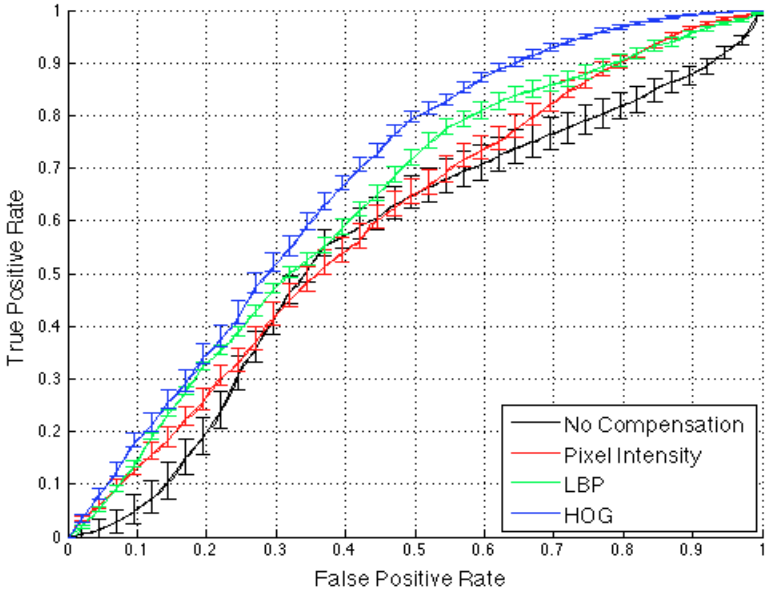

(a)

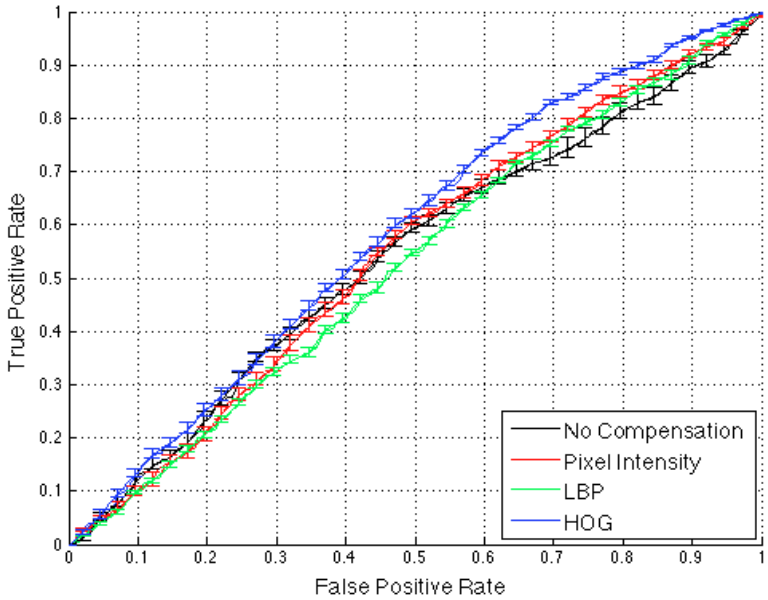

(b)

Values are expressed in boxplots, showing the median of the observed variations (horizontal solid line) and the first and third quartile values (top and bottom of the box marks). The horizontal lines outside each box denote the upper and lower whiskers, and dot points denote the outliers. By analysing these plots, it is obvious that the techniques proposed here for illumination and pose compensation contribute for consistent improvements in performance, as both the median and first and third quartile value are always positive, i.e., the variation in recognition sensitivity is clearly positive. The unique exception regards the case of *extremely deviated* data, where we concluded that the substantial amount of occluded data cannot be recovered by data projection techniques. In this case, we consider the problem insurmountable when imaging with a single camera. Even though, we concluded that the SQI contributes for improvements in sensitivity above seven percentile points, and the best pose optimisation variant (HOG) contributed for improvements in sensitivity around 13 percentile points, which was considered an achievement.

Figure 12 Summary of the improvements in recognition sensitivity (TPR) due to the use of the techniques proposed in this paper (see online version for colours)

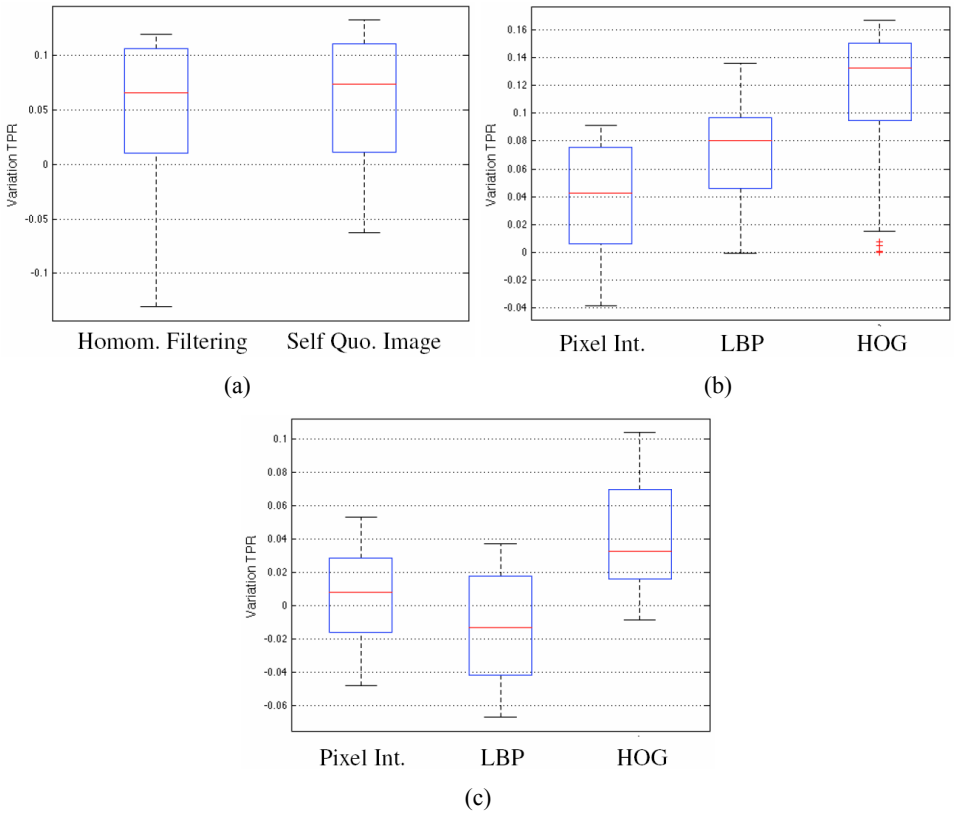

Notes: (a) the variations between the sensitivity values observed when using illumination compensation techniques and the observed without using any technique of this kind. Boxplots at (b) and (c) give the variations observed when using the pose compensation techniques described in this paper, with respect to not using any pose compensation technique.

Table 2 Comparison between the levels of performance obtained when using no pose compensation (denoted by no compensation) and the proposed compensation technique with the optimisation process that outperformed in our experiments (HOG-based)

# Samp. (# gen.–# imp.)		*510 (3,060–260,100)*			*765 (4,590–390,150)*			*255 (1,530–130,050)*		
Experiment	*AUC*	*Frontal*			*Deviated*			*Extremely deviated*		
		R	*L*	*R+L*	*R*	*L*	*R+L*	*R*	*L*	*R+L*
No compensation	HOG	0.687	0.715	0.743	0.637	0.707	0.686	0.549	0.527	0.539
	LBP	0.686	0.623	0.673	0.639	0.767	0.691	0.569	0.514	0.517
	SIFT	0.798	0.790	0.843	0.670	0.715	0.730	0.545	0.512	0.543
	Fusion	0.812	0.818	0.858	0.681	0.775	0.726	0.550	0.502	0.495
Prop. method	HOG	0.687	0.715	0.743	0.615	0.728	0.695	0.578	0.564	0.588
	LBP	0.686	0.623	0.673	0.628	0.761	0.705	0.580	0.578	0.589
	SIFT	0.798	0.790	0.843	0.694	0.745	0.763	0.555	0.539	0.563
	Fusion	0.812	0.818	0.858	0.693	0.784	0.764	0.534	0.433	0.554

When analysing the results with respect to each feature descriptor, the best performance was observed for the SIFT. This was explained by the fact of being a local descriptor and – as such – with potentially higher robustness to non-uniform (local) changes in illumination that are frequent in our dataset. Lastly, the results obtained for left eyes were consistently better than for right eyes, which was explained by specific conditions of the data acquisition environment, that determined that left eyes are often over-illuminated, in opposition to right eyes that tend to be under-illuminated and with more shadows.

9 Conclusions and future work

Growing efforts are concentrated in the robustness of periocular biometrics to covariates that result from relaxing the data acquisition constraints (such as misalignment between camera and subjects and varying illumination conditions). In this paper, we assessed the decreases in performance due to varying lighting conditions and subject's poses. Having confirmed the negative effects of both factors, we used homomorphic filters and SQIs to compensate for varying lighting conditions. Next, we described a method to compensate for pose based in a projective transform found from landmarks easily distinguishable in the periocular region (eye-corners), using a quadrilateral to maximise the similarity between gallery data and transformed probes. Our experiments pointed out that the proposed technique does not affect the results in case of frontal data and consistently improves performance when data is moderately deviated. Finally, we reported the maximal deviations that can be compensated with the proposed technique (up to 30°). For extremely deviated data (misalignments around 60° in terms of absolute value) substantial parts of the periocular region are occluded and – as the periocular region is far from planar – such missing information cannot be recovered by projection techniques derived from a single camera.

References

Abhyankar, A., Hornak, L. and Schuckers, S. (2005) 'Off-angle iris recognition using biorthogonal wavelet network system', in *Proceedings of the Fourth IEEE Workshop on Automatic Identification Advanced Technologies*, October, pp.239–244.

Bharadwaj, S., Bhatt, H., Vatsa, M. and Singh, R. (2010) 'Periocular biometrics: when iris recognition fails', in *Proceedings of the Fourth IEEE International Conference on Biometrics: Theory Applications and Systems (BTAS10)*, September, pp.1–6.

Chen, T., Wotao, Y., Xiang, S., Comaniciu, D. and Huang, T. (2006) 'Total variation models for variable lighting face recognition', *IEEE Transactions on Pattern Analysis and Machine Intelligence*, September, Vol. 28, No. 9, pp.1519–1524.

Cheng, Y., Jin, Z. and Hao, C. (2010) 'Illumination normalization based on different smoothing filters quotient image', in *Proceedings of the 3rd International Conference on Intelligent Networks and Intelligent Systems (ICINIS10)*, November, pp.28–31.

Cheung, K-W., Chen, J. and Moon, Y-S. (2008) 'Pose-tolerant non-frontal face recognition using EBGM', in *Proceedings of the 2nd IEEE International Conference on Biometrics: Theory, Applications and Systems (BTAS08)*, 29 2008–1 October 2008, pp.1–6.

Chou, C-T., Shih, S-W., Chen, W-S., Cheng, V. and Chen, D-Y. (2010) 'Non-orthogonal view iris recognition system', *IEEE Transactions on Circuits and Systems for Video Technology*, March, Vol. 20, No. 3, pp.417–430.

Crihalmeanu, S. and Ross, A. (2011) 'Multispectral scleral patterns for ocular biometric recognition', *Pattern Recognition Letters*, Vol. 33, No. 14, pp.1860–1869.

Dahmane, A., Larabi, S. and Djeraba, C. (2010) 'Detection and analysis of symmetrical parts on face for head pose estimation', in *Proceedings of the 17th IEEE International Conference on Image Processing (ICIP10)*, September, pp.3249–3252.

Demirel, H. and Anbarjafari, G. (2008) 'Pose invariant face recognition using probability distribution functions in different color channels', *Signal Processing Letters*, Vol. 15, pp.537–540.

Dorairaj, V., Schmid, N. and Fahmy, G. (2005) 'Performance evaluation of non-ideal iris based recognition system implementing global ICA encoding', in *Proceedings of the IEEE International Conference on Image Processing (ICIP05)*, pp.285–288.

Du, E.Y. and Yang, K. (2012) 'Speed-up multi-stage non-cooperative iris recognition', *International Journal of Biometrics*, Vol. 4, No. 4, pp.406–421.

Du, S. and Ward, R.K. (2010) 'Adaptive region-based image enhancement method for robust face recognition under variable illumination conditions', *IEEE Transactions on Circuits and Systems for Video Technology*, September, Vol. 20, No. 9, pp.1165–1175.

Gonzalez, R.C. and Woods, R.E. (1992) *Digital Image Processing*, Addison-Wesley Publishing Company, Boston, MA, USA.

González-Jiménez, D., Sukno, F., Alba-Castro, J. and Frangi, A. (2006) 'Automatic pose correction for local feature-based face authentication', in *Proceedings of the 4th International Conference on Articulated Motion and Deformable Objects (AMDO06), AMDO'06*, Springer-Verlag, Berlin, Heidelberg, pp.356–365.

He, X., Tian, J., Wu, L., Zhang, Y. and Yang, X. (2007) 'Illumination normalization with morphological quotient image', *Journal of Software*, Vol. 18, No. 9, pp.2318–2325.

Hollingsworth, K., Darnell, S., Miller, P., Woodard, D., Bowyer, K. and Flynn, P. (2012) 'Human and machine performance on periocular biometrics under near-infrared light and visible light', *IEEE Transactions on Information Forensics and Security*, April, Vol. 7, No. 2, pp.588–601.

Jia, J., Verma, A. and Liu, C. (2012) 'Iris recognition based on robust iris segmentation and image enhancement', *International Journal of Biometrics*, Vol. 4, No. 1, pp.56–76.

Juefei-Xu, F. and Savvides, M. (2012) 'Unconstrained periocular biometric acquisition and recognition using cots PTZ camera for uncooperative and non-cooperative subjects', in *Proceedings of the 2012 IEEE Workshop on Applications of Computer Vision (WACV12)*, January, pp.201–208.

Juefei-Xu, F., Luu, K., Savvides, M., Bui, T. and Suen, C. (2011) 'Investigating age invariant face recognition based on periocular biometrics', in *Proceedings of the International Joint Conference on Biometrics (IJCB11)*, October, pp.1–7.

Juhola, M., Zhang, Y. and Rasku, J. (2012) 'Biometric verification of subjects using saccade eye movements', *International Journal of Biometrics*, Vol. 4, No. 4, pp.317–337.

Kim, I-D., Lee, Y. and Shim, J-C. (2005) 'An automated facial pose estimation using surface curvature and tetrahedral structure of a nose', in *Advanced Concepts for Intelligent Vision Systems, Lecture Notes in Computer Science*, Springer Berlin/Heidelberg, Vol. 3708, pp.276–283.

Liu, X., Lu, H. and Luo, H. (2009) 'A new representation method of head images for head pose estimation', in *Proceedings of the 16th IEEE International Conference on Image Processing (ICIP09)*, November, pp.3585–3588.

Lyle, J.R., Miller, P.E., Pundlik, S.J. and Woodard, D.L. (2010) 'Soft biometric classification using periocular region features', in *Proceedings of the Fourth IEEE International Conference on Biometrics: Theory Applications and Systems (BTAS10)*, September, pp.1–7.

Miller, P., Lyle, J., Pundlik, S. and Woodard, D. (2010) 'Performance evaluation of local appearance based periocular recognition', in *Proceedings of the Fourth IEEE International Conference on Biometrics: Theory Applications and Systems (BTAS10)*, September, pp.1–6.

Murphy-Chutorian, E. and Trivedi, M. (2009) 'Head pose estimation in computer vision: a survey', *IEEE Transactions on Pattern Analysis and Machine Intelligence*, April, Vol. 31, No. 4, pp.607–626.

NIST, 'Face recognition grand challenge database' [online] http://www.nist.gov/itl/iad/ig/frgc.cfm (accessed 10/05/2013).

Padole, C. and Proença, H. (2012) 'Periocular recognition: analysis of performance degradation factors', in *Proceedings of the Fifth IEEE International Conference on Biometrics (ICB 2012)*, March, pp.1–6.

Park, U., Jillela, R., Ross, A. and Jain, A.K. (2011) 'Periocular biometrics in the visible spectrum', *IEEE Transactions on Information Forensics and Security*, March, Vol. 6, No. 1, pp.96–106.

Park, U., Ross, A. and Jain, A.K. (2009) 'Periocular biometrics in the visible spectrum: a feasibility study', in *Proceedings of the IEEE 3rd International Conference on Biometrics: Theory, Applications, and Systems (BTAS09)*, September, pp.1–6.

Park, U., Ross, A. and Jain, A.K. (2012) 'Matching highly non-ideal ocular images: an information fusion approach', in *Proceedings of the IEEE 5th International Conference on Biometrics (ICB12)*, March.

Paul, S. (1989) *Fundamental of Texture Mapping and Image Warping*, Master Thesis, University of California, Berkeley.

Proença, H., Filipe, S., Santos, R., Oliveira, J. and Alexandre, L.A. (2010) 'The ubiris.v2: a database of visible wavelength iris images captured on-the-move and at-a-distance', *IEEE Transactions on Pattern Analysis and Machine Intelligence*, August, Vol. 32, No. 8, pp.1529–1535.

Santos, G. and Proença, H. (2011) 'A robust eye-corner detection method for real-world data', *Proceedings of the International Joint Conference on Biometrics (IJCB11)*, pp.1–7.

Savvides, M., Ricanek, K., Woodard, D. and Dozier, G. (2010) 'Unconstrained biometric identification: emerging technologies', *Computer*, Vol. 43, pp.56–62.

Schmid, N., Kalka, N., Zuo, J. and Cukic, B. (2010) 'Estimating and fusing quality factors for iris biometric', *IEEE Transactions on Systems, Man, and Cybernetics: Part A*, Vol. 40, No. 3, pp.509–524.

Schuckers, S., Schmid, N., Abhyankar, A., Dorairaj, V., Boyce, C.K. and Hornak, L. (2007) 'On techniques for angle compensation in non-ideal iris recognition', *IEEE Transactions on Systems, Man, and Cybernetics, Part B: Cybernetics*, October, Vol. 37, No. 5, pp.1176–1190.

Selvan, S. and Sulochana, C.H. (2010) 'Robust iris recognition algorithm for non-cooperative environment', *International Journal of Biometrics*, Vol. 2, No. 1, pp.71–86.

Shashua, A. and Riklin-Raviv, T. (2001) 'The quotient image: classbased re-rendering and recognition with varying illuminations', *IEEE Transactions on Pattern Analysis and Machine Intelligence*, Vol. 23, No. 2, pp.129–139.

Simpson, L., Dozier, G., Adams, J., Woodard, D.L., Miller, P., Bryant, K. and Glenn, G. (2010) 'Genetic amp; evolutionary type ii feature extraction for periocular-based biometric recognition', in *Proceedings of the IEEE Congress on Evolutionary Computation (CEC10)*, July, pp.1–4.

Singh, R., Vatsa, M., Ross, A. and Noore, A. (2007) 'A mosaicing scheme for pose-invariant face recognition', *IEEE Transactions on Systems, Man, and Cybernetics, Part B: Cybernetics*, October, Vol. 37, No. 5, pp.1212–1225.

Srividya, T., Arivazhagan, S. and Ganesan, L. (2009) 'Iris recognition using multi-resolution transforms', *International Journal of Biometrics*, Vol. 1, No. 3, pp.254–267.

Storer, M., Urschler, M. and Bischof, H. (2009) '3d-mam: 3d morphable appearance model for efficient fine head pose estimation from still images', in *Proceedings of the IEEE 12th International Conference on Computer Vision Workshops (ICCV09 Workshops)*, October, pp.192–199.

Thangasamy, S. and Latha, L. (2012) 'Efficient method of person authentication based on fusion of best bits in left and right irises', *International Journal of Biometrics*, Vol. 4, No. 3, pp.203–219.

Wang, H., Li, S. and Wang, Y. (2004) 'Generalized quotient image', in *Proceedings of the 2004 Conference on Computer Vision and Pattern Recognition (CVPR04)*, Vol. 2, pp.498–505.

Wang, H., Liu, J. and Wang, Y. (2005) 'Self-quotient image', *Computer Engineering*, Vol. 31, No. 18, pp.178–179.

Wolf, L., Hassner, T. and Taigman, Y. (2011) 'Effective unconstrained face recognition by combining multiple descriptors and learned background statistics', *IEEE Transactions on Pattern Analysis and Machine Intelligence*, October, Vol. 33, No. 10, pp.1978–1990.

Woodard, D., Pundlik, S., Miller, P. and Lyle, J. (2011) 'Appearance-based periocular features in the context of face and non-ideal iris recognition', *Signal, Image and Video Processing*, Vol. 5, pp.443–455, 10.1007/s11760-011-0248-2.

Woodard, D.L., Pundlik, S., Miller, P., Jillela, R. and Ross, A. (2010) 'On the fusion of periocular and iris biometrics in non-ideal imagery', in *Proceedings of the 20th International Conference on Pattern Recognition (ICPR10)*, August, pp.201–204.

Wu, J. and Trivedi, M. (2008) 'A two-stage head pose estimation framework and evaluation', *Pattern Recognition, Special issue on Feature Generation and Machine Learning for Robust Multimodal Biometrics*, August, Vol. 41, No. 3, pp.1138–1158.

Xie, X., Zheng, W-S., Lai, J. and Yuen, P. (2008) 'Face illumination normalization on large and small scale features', in *Proceedings of the IEEE Conference on Computer Vision and Pattern Recognition (CVPR08)*, June, pp.1–8.

Xie, X., Zheng, W-S., Lai, J., Yuen, P. and Suen, C. (2011) 'Normalization of face illumination based on large-and small-scale features', *IEEE Transactions on Image Processing*, July, Vol. 20, No. 7, pp.1807–1821.

Zhao, S. and Gao, Y. (2006) 'Automated face pose estimation using elastic energy models', in *Proceedings of the18th International Conference on Pattern Recognition, (ICPR06)*, August, Vol. 4, pp.618–621.

Zheng, W., Tang, H., Lin, Z. and Huang, T. (2009) 'A novel approach to expression recognition from non-frontal face images', in *Proceedings of the IEEE International Conference on Computer Vision (ICCV09)*, pp.1901–1908.

Zuo, J. and Schmid, N. (2009) 'Global and local quality measures for NIR iris video', in *Proceedings of the IEEE International Conference on Computer Vision and Pattern Recognition (CVPR09)*, pp.120–125.

Notes

1 http://socia-lab.di.ubi.pt/~ubiposepr.